Chemical Shift Correlations from Hyperpolarized NMR using a single SHOT

ARTICLE *in* ANALYTICAL CHEMISTRY · JANUARY 2013

Impact Factor: 5.64 · DOI: 10.1021/ac303313s

4 AUTHORS, INCLUDING:

Guannan Zhang
Texas A&M University
2 PUBLICATIONS **9** CITATIONS
SEE PROFILE

Franz Schilling
University of Cambridge
19 PUBLICATIONS **62** CITATIONS
SEE PROFILE

Christian Hilty
Texas A&M University
64 PUBLICATIONS **1,765** CITATIONS
SEE PROFILE

analytical chemistry

Article

pubs.acs.org/ac

Chemical Shift Correlations from Hyperpolarized NMR Using a Single SHOT

Guannan Zhang,[†,§] Franz Schilling,[‡,§] Steffen J. Glaser,[‡] and Christian Hilty*[,†]

[†]Department of Chemistry, Texas A&M University, 3255 TAMU, College Station, Texas 77843-3255, United States

[‡]Department of Chemistry, Technische Universität München, 85747 Garching, Germany

Supporting Information

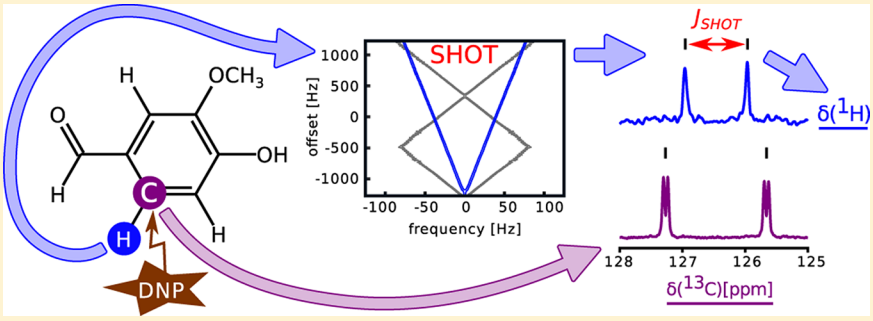

ABSTRACT: A significant challenge in realizing the promise of the dissolution dynamic nuclear polarization technique for signal enhancement in high-resolution NMR lies in the nonrenewability of the hyperpolarized spin state. This property prevents the application of traditional two-dimensional correlation spectroscopy, which relies on regeneration of spin polarization before each successive increment of the indirect dimension. Since correlation spectroscopy is one of the most important approaches for the identification and structural characterization of molecules by NMR, it is important to find easily applicable methods that circumvent this problem. Here, we introduce the application of scaling of heteronuclear couplings by optimal tracking (SHOT) to achieve this goal. SHOT decoupling pulses have been numerically optimized on the basis of optimal control algorithms to obtain chemical shift correlations in C−H groups, either by acquiring a single one-dimensional ^{13}C spectrum with ^{1}H off-resonance decoupling or vice versa. Vanillin, which contains a number of functional groups, was used as a test molecule, allowing the demonstration of SHOT decoupling tailored toward simplified and accurate data analysis. This strategy was demonstrated for two cases: First, a linear response to chemical shift offset in the correlated dimension was optimized. Second, a pulse with alternating linear responses in the correlated dimension was chosen as a goal to increase the sensitivity of the decoupling response to the chemical shift offset. In these measurements, error ranges of ±0.03 ppm for the indirectly determined ^{1}H chemical shifts and of ±0.4 ppm for the indirectly determined ^{13}C chemical shifts were found. In all cases, we show that chemical shift correlations can be obtained from information contained in a single scan, which maximizes the ratio of signal to stochastic noise. Furthermore, a comprehensive discussion of the robustness of the method toward nonideal conditions is included based on experimental and simulated data. Unique features of this technique include the abilities to control the accuracy of chemical shift determination in spectral regions of interest and to acquire such chemical shift correlations rapidly—the latter being of interest for potential application in real-time spectroscopy.

Dissolution dynamic nuclear polarization (DNP) has in recent years gained considerable popularity for enhancing the signal in magnetic resonance experiments by orders of magnitude.[1] Using this technique, nuclear spins of a sample aliquot are hyperpolarized by transfer of polarization from electron spins at cryogenic temperature. Subsequent dissolution yields liquids containing analytes with a large, nonequilibrium nuclear spin polarization. The gain in signal from this nonequilibrium polarization has the potential to impart significant benefits for the analysis of mass-limited samples of natural or synthetic origin.[2] Furthermore, the absence of signal averaging reduces the time requirement for obtaining high-quality NMR spectra to the Nyquist limit, pushing the boundary of NMR for the determination of kinetics and intermediate species in chemical reactions.[3]

A challenge in the application of dissolution DNP to problems in chemistry lies in the fact that modern NMR techniques for the structural analysis or simply the identification of compounds heavily rely on correlation spectroscopy. In all but the simplest cases, chemical shift correlations between neighboring spins are essential to establish the connectivity of atoms in a molecule. Conventionally, homonuclear or heteronuclear correlations are obtained from

Received: December 1, 2012
Accepted: January 24, 2013

   dx.doi.org/10.1021/ac303313s | *Anal. Chem.* XXXX, XXX, XXX−XXX

two-dimensional (2D) experiments, using chemical shift evolution in an indirect dimension followed by coherence transfer between the two atoms.[4] The acquisition of a 2D spectrum requires the repetition of the experiment for various evolution times. It is therefore not directly applicable to a single hyperpolarized sample from dissolution DNP, since in this case the hyperpolarization is lost after application of a single excitation pulse with flip angle $\pi/2$.

Several strategies exist to recover information from spin correlations that are applicable to dissolution DNP. True 2D spectroscopy can be carried out using ultrafast, single-scan techniques[5,6] or using sequential scanning of the second dimension with small-flip-angle excitation.[7] A different way of obtaining heteronuclear chemical shift correlations without the need for acquiring a full indirect spectral dimension is through off-resonance decoupling. In off-resonance decoupling, a radio frequency field is applied at the frequency of one type of nucleus (for example, ^{1}H) during the acquisition of a one-dimensional spectrum of a second type of nucleus (for example, ^{13}C). If the decoupling field is of sufficiently low amplitude, an effective residual scalar coupling remains observable for spins that are off-resonance from the decoupling field. From the magnitude of this residual coupling, it is possible to back-calculate the difference in chemical shift between the irradiation frequency and the actual frequency of the coupled spin.

Off-resonance continuous wave (CW) decoupling has been studied since the early days of NMR[8,9] and was introduced as a means of obtaining correlation information prior to the advent of 2D NMR.[10] More recently, it has been used extensively for chemical shift monitoring in pseudomultidimensional biomolecular NMR experiments, where dimensionality can be increased without the need for the time-consuming process of acquiring an additional dimension.[11−15] Previously, our group proposed the use of off-resonance CW decoupling in conjunction with dissolution DNP.[16] An advantage of the technique in this context is that correlation information can be reconstructed from a small set of spectra. Even though off-resonance CW decoupling does not resolve signal overlap, for small molecules that are often the target of dissolution DNP experiments, this is often not an issue.

In CW off-resonance decoupling, the effective scaling of the scalar coupling constant is a nonlinear function of frequency offset.[17] As a result, the accuracy of the back-calculated chemical shift for any given spin is strongly dependent on the chosen decoupling frequency. In a typical case, acquisition of at least three or four spectra with different decoupling frequencies is required for reliable reconstruction of all chemical shifts in a molecule. Unfortunately, splitting the polarization from a single hyperpolarized sample into multiple spectra results in the acquisition of independent noise in each scan. Additionally, the time required for the acquisition of multiple scans reduces the utility of the method for use in real-time spectroscopy.

In remedy of these shortfalls, recently, a method allowing for an arbitrarily chosen offset dependence of the effective coupling constant has been developed.[18] Scaling of heteronuclear couplings by optimal tracking (SHOT) refers to the numerical optimization of a decoupling pulse based on optimal control algorithms,[18−20] which is then applied synchronously during the data acquisition to provide a predefined offset dependence in the effective coupling constant. This robust approach can take B_1 inhomogeneities into account and can create virtually arbitrary offset profiles of the effective coupling constant. SHOT pulses can thereby overcome limitations that have been imposed to chemical shift encoding via off-resonance CW decoupling, most importantly solving the problems of nonlinear chemical shift dependence of the residual coupling and the sensitivity toward B_1 miscalibrations. In contrast to band-selective decoupling pulses with a scaling factor of either 0 or 1 in defined offset ranges,[21−25] SHOT pulses are entirely optimized de novo and give the experimentalist the opportunity to tailor the decoupling offset profiles to the specific needs of the molecule under investigation. Here, we demonstrate that off-resonance decoupling with such tailored pulses provides significant advantages for the rapid, accurate, and sensitive detection of chemical shift correlations by dissolution DNP.

EXPERIMENTAL SECTION

SHOT pulses were optimized to cover the chemical shift range and J coupling values of the vanillin molecule. For covering all coupled spins, a decoupling bandwidth (BW) of 2500 Hz is needed for protons and a BW of 15 000 Hz is needed for carbons. Optimizations of the pulses were performed with a MATLAB script (The Mathworks, Natick, MA), which is available from the authors upon request. The goal of each optimization is to trace the scaling of the J coupling constant chosen for the optimization, J_{opt}, over a range of offset frequencies and match it to a well-defined target profile, $J_{SHOT}(\nu)$.[18] The desired profile functions were discretized by Z offset frequencies separated by BW/Z between two offset points for the optimization algorithm. In all cases, optimization was carried out using an assumed value of the heteronuclear coupling constant, J_{opt} = 160 Hz, in the absence of off-resonance decoupling. This value corresponds to an approximate average of coupling constants observed in vanillin, which range from 145 Hz (methoxy group) to 174 Hz (aldehyde group). Pulses were designed to be robust to miscalibrations in radio frequency (rf) amplitude ($\gamma B_1/2\pi$) of ±2%. Furthermore, we assumed an effective relaxation rate constant (κ) of 18.8 s^{-1}, corresponding to an experimental line width of 6 Hz. The resulting SHOT pulses, which were synchronized with receiver sampling, were digitized by $N \cdot M$ pairs of values for amplitude and phase. Here, N corresponds to the number of acquisiton points in the pulse optimization and M corresponds to the number of amplitude and phase modulations between two successive acquisition points. A library of the SHOT pulses used in this work has been made available for download.[26] Details about implementation of SHOT pulses on the spectrometer can be found in the Supporting Information.

For proton decoupling, pulses with a linear offset dependence of the residual coupling constant

$$J_{SHOT}(\nu) = J_{opt}\frac{\nu + \nu_{max}}{2\nu_{max}} \quad (1)$$

and a profile consisting of three linear segments of successively reversed direction ("zigzag profile")

dx.doi.org/10.1021/ac303313s | Anal. Chem. XXXX, XXX, XXX−XXX

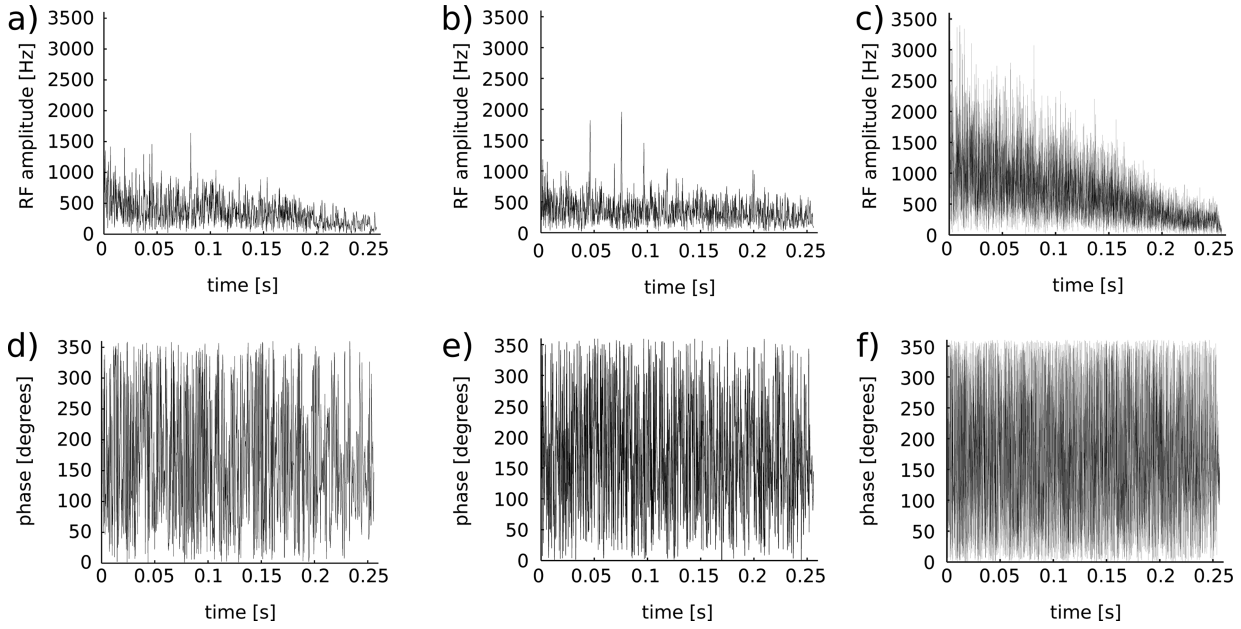

Figure 1. Pulse amplitudes for the (a) linear proton decoupling pulse, (b) zigzag proton decoupling pulse, and (c) linear carbon decoupling pulse. (d), (e), and (f) are the pulse phases for the pulses in (a), (b), and (c), respectively.

$$J_{\mathrm{SHOT}}(\nu) = \begin{cases} J_{\mathrm{opt}}\dfrac{\nu + \nu_{\max}}{800\ \mathrm{Hz}} & -\nu_{\max} < \nu \\ & \leq -450\ \mathrm{Hz} \\ J_{\mathrm{opt}}\left(1 - \dfrac{\nu + 425\ \mathrm{Hz}}{800\ \mathrm{Hz}}\right) & -425\ \mathrm{Hz} \\ & < \nu \leq +375\ \mathrm{Hz} \\ J_{\mathrm{opt}}\dfrac{\nu - 400\ \mathrm{Hz}}{800\ \mathrm{Hz}} & 400\ \mathrm{Hz} < \nu \leq \nu_{\max} \end{cases} \tag{2}$$

were calculated. The maximum positive or negative frequency offset from the transmitter frequency (ν), for which both of the pulses are valid, is $\nu_{\max}$ = BW/2 = 1250 Hz. For the zigzag profile, there is a 25 Hz break between two piecewise defined regions originating from the finite offset discretization, which was set to Z = 101 for both pulses. Additional parameters are N = 128 and M = 10. The maximum rf amplitudes for the linear pulse and zigzag pulse are $(\gamma/2\pi)B_{1,\max}$ = 1.64 kHz and $(\gamma/2\pi)B_{1,\max}$ = 1.96 kHz. For carbon SHOT decoupling, a linear offset profile according to eq 1 was chosen with $\nu_{\max}$ = BW/2 = 7500 Hz. Additional parameters are Z = 301, N = 1024, and M = 10. The pulse amplitude is $(\gamma/2\pi)B_{1,\max}$ = 3.51 kHz. The amplitude and phase pattern for both of the proton and carbon decoupling pulses are shown in Figure 1. In all cases, a total acquisition time (T) of 256 ms was used.

The SHOT pulses yielded simulated frequency profiles that closely match the predefined functions in eqs 1 and 2 (Figure 2). On the basis of these profiles, the effective coupling constant under SHOT decoupling, J_{SHOT}, varies linearly (or, in the case of the zigzag pulse, segmentally linearly) with offset. Furthermore, experimental decoupling profiles were measured by conventional (i.e., not hyperpolarized) NMR, using a concentrated sample of vanillin and stepping through different transmitter frequency offset settings. Parts b and d of Figure 2 compare these experimental data points with curves drawn from the original equations. For both the linear and zigzag patterns, the experimentally determined points are in good agreement with the theoretical curve despite the fact that the

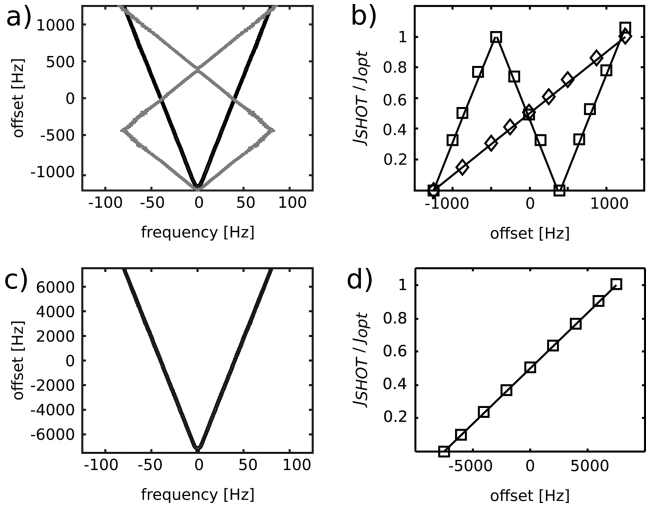

Figure 2. (a) Contour plot showing the simulated off-resonance coupling pattern of the zigzag (gray lines) and linear (black lines) SHOT pulses for ^{1}H decoupling as a function of the transmitter offset frequency, calculated for 501 offsets within the bandwidth and applying a zero-filling factor of 10. Contour levels are shown for 95% of the maximum peak amplitude in the 1D spectrum for each offset. (b) ^{1}H off-resonance pattern functions determined from eqs 1 and 2 (solid lines) and measured using nonhyperpolarized NMR from the aldehyde group, which shows an actual coupling constant of 174 Hz. (c) Simulation of the ^{13}C off-resonance decoupling profile as in (a), but calculated for 1001 offsets. (d) Linear off-resonance pattern function as in (b), but for ^{13}C decoupling.

actual coupling constant for the C−H group, which is 174 Hz, is 14 Hz larger than the assumed coupling constant J_{opt} = 160 Hz.

Even though these pulses have been optimized for the vanillin molecule, the only specific information used was (1) the J coupling constant J_{opt}, which should be chosen in the range of the actual J couplings for reduction of sidebands, (2) the transmitter frequency range which was matched to the

dx.doi.org/10.1021/ac303313s | Anal. Chem. XXXX, XXX, XXX−XXX

proton/carbon chemical shifts, and (3) the off-resonance-dependent decoupling pattern, which can be chosen arbitrarily.

Dynamic Nuclear Polarization and NMR Spectroscopy. The DNP experiment requires selection of two solvents, the glass-forming solvent for DNP in the solid state and the dissolution solvent for transferring the frozen sample into the preinstalled NMR tube. A DMSO/water mixture was chosen for the glass-forming solvent to avoid peak overlap with the ^{13}C spectrum of vanillin. For the dissolution, the low-viscosity solvent acetonitrile was used to facilitate sample injection. Samples for hyperpolarization consisted of 10 μL of 2 M vanillin dissolved in 72% DMSO and 28% H_2O for ^{13}C experiments or 72% DMSO-d_6 and 28% D_2O for ^{1}H experiments. All samples contained 15 mM tris[8-carboxy-2,2,6,6-tetrakis(2-hydroxyethyl)benzo[1,2-*d*:4,5-*d*′]bis[1,3]-dithiol-4-yl]methyl free radical sodium salt (OX63; Oxford Instruments, Tubney Woods, U.K.) for ^{13}C experiments or 4-hydroxy-2,2,6,6-tetramethylpiperidine-1-oxyl (TEMPOL) free radical (Sigma-Aldrich, St. Louis, MO) for ^{1}H experiments. Samples were hyperpolarized on ^{13}C in a HyperSense DNP polarizer (Oxford Instruments) by irradiation with 60 mW power at a frequency of 93.974 GHz ($\omega_e - \omega_N$) for 3 h at a temperature of 1.4 K. Hyperpolarization on ^{1}H was carried out using a frequency of 94.005 GHz ($\omega_e - \omega_N$), a power of 100 mW, and an irradiation time of 30 min. The hyperpolarized samples were dissolved in preheated acetonitrile and transferred to a 5 mm NMR tube installed in a 400 MHz NMR spectrometer with a modified broad-band observe (BBO) probe (Bruker Biospin, Billerica, MA), using a rapid sample injection device described elsewhere.[27] Pressurized nitrogen gas of 17.2 and 10.3 bar for forward and backward pressures, respectively, was applied during sample injection. The total time elapsed from the beginning of the injection to the start of the NMR measurement (excluding time for loading sample loop) was 770 ms for the ^{13}C detected experiments and 1.85 s for the ^{1}H detected experiments.

The pulse sequences used for acquisition of off-resonance decoupled spectra have been described previously (see also the Supporting Information).[16] A reference scan and a SHOT decoupled spectrum were acquired from each hyperpolarized sample, using variable small-flip-angle excitation.[7] During acquisition of the second scan, a SHOT decoupling pulse (for parameters see above) was applied. For the ^{13}C detected experiment, the free induction decay was digitized with 12 800 complex points (10× the number of digitization points in the SHOT pulse). The transmitter frequency offset from 0 ppm was 2670.23 Hz for the ^{1}H decoupling channel. A conventional ^{1}H spectrum was obtained immediately after each hyperpolarized ^{13}C experiment to verify the actual proton chemical shifts under the same experimental conditions. For the ^{1}H detected experiment, a filter element was applied to remove unwanted signal from spins not coupled to ^{13}C. The number of complex points in the free induction decay was 10 240, and the transmitter frequency offset from 0 ppm was 13 134.02 Hz for the ^{13}C decoupling channel. Chemical shifts of ^{1}H of both the hyperpolarized and conventional experiments were referenced to the solvent resonance of acetonitrile. The chemical shift of acetonitrile was calibrated to tetramethylsilane (TMS) at 0 ppm using the substitution method. Chemical shifts of ^{13}C were indirectly calibrated via the known ^{1}H calibration, using $\gamma_C/\gamma_H = 0.251\,450\,20$.[28] Since this frequency ratio is based on a different solvent, we expect a small offset from the actual carbon chemical shift. This offset is however identical for decoupled and undecoupled experiments, so it does not introduce an error for the comparisons.

RESULTS AND DISCUSSION

The performance of SHOT pulses for obtaining chemical shift correlations from hyperpolarized samples by both proton and carbon off-resonance decoupling was evaluated using model samples of approximately 0.3 mM vanillin, with natural (1.1%) abundance of ^{13}C. Vanillin contains a number of diverse functional groups with different chemical shifts and coupling constants. Additionally, the choice of vanillin for these experiments permits the direct comparison of results with CW off-resonance decoupling.[16]

Spectra obtained with each of the three decoupling pulses are shown in Figure 3. Comparing the SHOT decoupled upper trace with the undecoupled lower trace in each panel confirms that the coupling constant is reduced by different amounts for each peak. Despite acquisition of the decoupled spectra as the second scan, the height of some peaks is larger in the ^{1}H SHOT decoupled spectra than in undecoupled spectra due to serendipitous removal of long-range $^{1}H-^{13}C$ couplings. This feature further enhances the ratio of signal to stochastic noise in the SHOT decoupled experiment.

Since the linear SHOT pulses for proton or carbon decoupling cover the full frequency range of coupled proton or carbon spins, all heteronuclear chemical shift correlations can be unambiguously back-calculated from a single one-dimensional spectrum with SHOT decoupling (eq 1). In the case of the zigzag pulse for proton decoupling, chemical shifts can also be calculated from a single spectrum, as long as it is known which of the three intervals a chemical shift falls into. This knowledge may, for example, be inferred from the known carbon chemical shift, or it may be given if observing chemical shift changes in known compounds. The zigzag SHOT pulse provides the advantage that the slope $\Delta J_{SHOT}/\Delta\nu$ is larger than in the case of the linear pulse, hence theoretically resulting in a higher sensitivity of the determined chemical shift with respect to the measured coupling constant.

In an expanded view of the obtained peaks (Figures 3 and S1, Supporting Information), the residual coupling constants J_{SHOT} can readily be measured. Chemical shift correlations can thus be obtained from either a ^{13}C or a ^{1}H detected experiment. Which one of those options is more favorable will be dependent on the individual problem. ^{13}C hyperpolarization and detection offers the advantage of a large chemical shift dispersion, which helps reduce signal overlap. In fact, in the proton detected spectrum, peaks 5 and 7 partially overlap, and in addition peak 5 is split into a doublet due to long-range proton−proton coupling. This overlap introduces more error in the calculation of the carbon chemical shift for atom 7. Carbon detection can also be favorable because ^{13}C nuclei often show relatively long spin−lattice relaxation times, which aids in the preservation of hyperpolarization. On the other hand, the largest absolute signal may be obtained from ^{1}H due to its near 100% natural abundance and large gyromagnetic ratio.

Chemical shifts were calculated from the spectra in Figure 3 for all peaks as $10^6(\nu_{trans} + \nu)/\nu_0$, where ν_0 is the frequency corresponding to 0 ppm on the decoupling channel, ν_{trans} is the decoupler offset from ν_0, and ν is derived from eqs 1 and 2 (see Tables S1 and S2 in the Supporting Information). For the calculation, it was assumed that the actual coupling constant for each spin pair is J_{opt} = 160 Hz. To evaluate the accuracy of this method, it may be most useful to compare the back-calculated

dx.doi.org/10.1021/ac303313s | Anal. Chem. XXXX, XXX, XXX−XXX

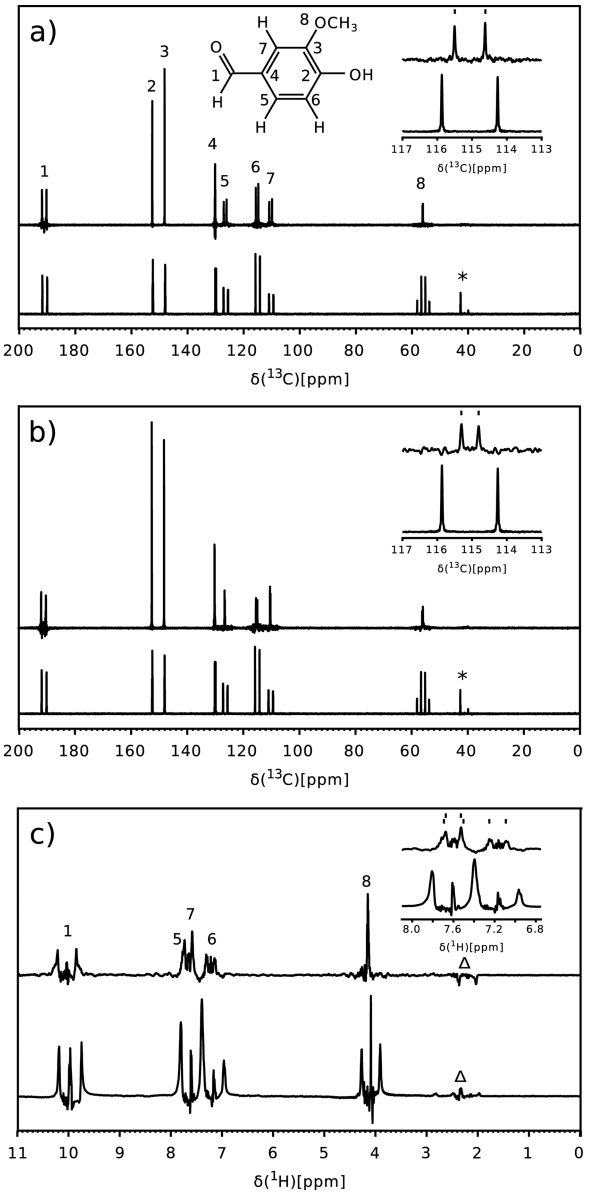

Figure 3. (a) Spectrum of ^{13}C hyperpolarized vanillin with ^{1}H SHOT decoupling using the pulse with a linear profile (top) and reference spectrum without decoupling (bottom). Decoupled and reference spectra were acquired from a single hyperpolarized sample. (b) Spectra as in (a), but acquired with a zigzag SHOT pulse. (c) Spectrum of ^{1}H hyperpolarized vanillin with ^{13}C SHOT decoupling. In all data sets, the bottom spectra were acquired first using a $\pi/4$ excitation pulse, followed by the top spectra with a $\pi/2$ pulse. The asterisks designate resonances from the partially suppressed solvent peak for DMSO in (a) and (b), and triangles designate resonances from the unsuppressed dissolution solvent peak for acetonitrile. Three panels of the expanded views for peak 6 corresponding to (a) and (b) and peaks 5, 7, and 6 corresponding to (c) are shown.

chemical shifts to the actual chemical shifts obtained from a ^{1}H (^{13}C) or ^{13}C (^{1}H) spectrum of a vanillin sample under similar conditions. Figure 4 contains plots that show this error both as a function of frequency offset from the SHOT irradiation frequency and as a deviation in the coupling constant from the average coupling of 160 Hz. It is apparent that the error of the calculated chemical shift is within ±0.03 ppm for indirectly determined ^{1}H chemical shifts and within ±0.4 ppm for indirectly determined ^{13}C chemical shifts. Since the accuracy of

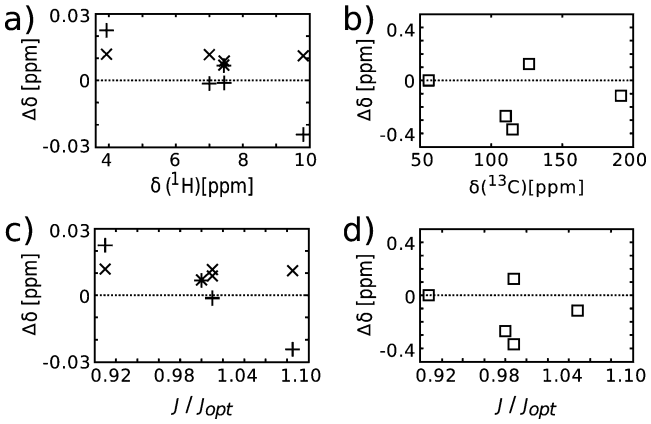

Figure 4. (a) Chemical shift error $\Delta\delta$ of back-calculation from the ^{13}C detected experiment with ^{1}H decoupling using the linear SHOT pulse and the zigzag SHOT pulse, designated by "+" and "×", and shown as a function of the actual chemical shift. (b) Chemical shift error of a ^{1}H detected experiment with ^{13}C decoupling using the linear SHOT pulse. (c, d) Data from (a) and (b), but shown as a function of the actual coupling constant J over J_{opt}.

the back-calculated chemical shift depends on the slope of the offset function pattern, use of the zigzag pulse is potentially advantageous. When comparing the spread of chemical shift errors ($\Delta\delta$) of the two pulses, the zigzag SHOT does appear to give overall smaller error than the linear SHOT. From the data in Figure 4, no conclusive correlation between the chemical shift error and absolute chemical shift or deviation of the actual from the assumed coupling constant can be identified; SHOT pulses appear to perform relatively uniformly over these parameter ranges.

In contrast, CW off-resonance decoupling suffers increased inaccuracy for large offsets, where the effective coupling constant asymptotically approaches the true coupling constant. Using CW decoupling, spectra with decoupling at up to four different chemical shift offsets plus one reference spectrum are required.[16] The ratio of the signal to the stochastic noise floor is reduced by 5-fold (not considering relaxation losses). In the SHOT experiment, the linear dependence of $J_{SHOT}(\nu)$ on offset allows for simplified back-calculation of chemical shifts, while requiring the distribution of hyperpolarized magnetization into fewer scans. If coupling constants in a certain range of the molecule under investigation are scaled to an off-resonance pattern by an optimized SHOT pulse and the range of coupling constants is known, the reference spectra shown in Figure 3 are not needed for calculation of chemical shift correlations. A single spectrum with SHOT decoupling is then sufficient for calculation of the chemical shift.

In the SHOT decoupled experiments (Figures 3 and S1, Supporting Information), decoupling sidebands are visible in all cases near the partially decoupled peaks. Such sidebands produced by SHOT decoupling pulses are a systematic noise source and have been previously reported. However, sidebands can be simulated with good accuracy for a given SHOT pulse.[18] Since here the decoupled signal amplitudes are well above the sideband amplitudes, they do not limit the determination of chemical shift correlations. In the ^{1}H spectra, a further peak is visible in the center of each multiplet due to incomplete suppression of the large signal from protons not coupled to ^{13}C.

The reduction in the signal to systematic noise ratio due to such artifacts is balanced by the reduced amount of loss due to

dx.doi.org/10.1021/ac303313s | Anal. Chem. XXXX, XXX, XXX−XXX

relaxation of later scans in CW off-resonance decoupling or other experiments involving the sequential acquisition of multiple scans. Compared to sequentially acquired 2D spectra obtained from hyperpolarized samples,[7] this effect is even more substantial due to the need for a large number of points in the indirect dimension (e.g., 32) in the 2D spectra. Single-scan ultrafast 2D spectroscopy, where the hyperpolarized magnetization is distributed and read out in separate subvolumes of the sample, does not suffer from this problem, but a noise penalty still has to be paid because of the required increase in receiver bandwidth.[5] In contrast, SHOT decoupling uses all magnetization in the sample by encoding chemical shift correlations only through the chemical shift dependent scaled splitting of the J couplings. Off-resonance decoupling in its simplest form (for example, using ^{13}C acquisition) further does not require the application of pulsed field gradients, avoiding the potential for signal loss due to incomplete refocusing.[29] Even in the case of a carbon filter, only sparing use of pulsed field gradients is made.

In addition to the experimental demonstration of the SHOT decoupling pulses with hyperpolarization, we performed simulations to assess the robustness of the method with respect to various deviations from ideal behavior. Foremost, the SHOT pulses used here have been calculated for an average coupling constant J_{opt} = 160 Hz. However, actual $^{1}H-^{13}C$ coupling constants in our test molecule vanillin and in typical other molecules may range from approximately 145 to 174 Hz. Figure 5 compares simulations of offset-dependent decoupling profiles under the assumption of different coupling constants. Figure 5a shows an artifact that limits the chemical shift resolution due to truncation of the free induction decay (FID) at an acquisition time of 256 ms, yielding a frequency resolution of 3.9 Hz. The resulting step pattern is clearly visible, but the effect can be alleviated by zero-filling with a factor of 10, as applied for the other panels.

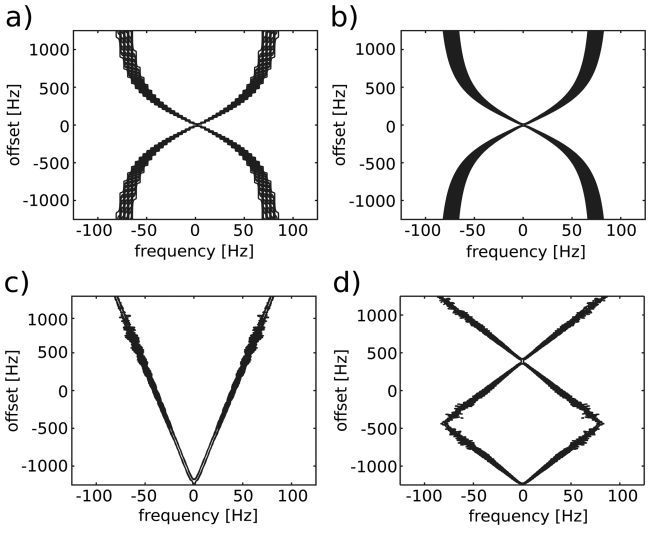

Figure 5. Simulation of off-resonance decoupling profiles for a range of actual coupling constants, J = 145−174 Hz. (a) CW pulse with rf amplitude $(\gamma/2\pi)B_{1,max}$ = 0.50 kHz and a dwell time of 256 ms/1280. (b) CW pulse as in (a), but using a zero-filling factor of 10 for data processing. (c) Linear SHOT pulse for protons, with $(\gamma/2\pi)B_{1,RMS}$ = 0.43 kHz and a zero-filling factor of 10. (d) Zigzag SHOT pulse for protons, with $(\gamma/2\pi)B_{1,RMS}$ = 0.42 kHz and a zero-filling factor of 10. All contour plots show contour levels at 95% of the maximum peak amplitude in each 1D spectrum and its corresponding offset. Spectra were simulated for 501 offsets in a frequency offset range of 2500 Hz.

In Figure 5, the spreads of observed residual coupling constants for spin systems with J in the range between 145 and 174 Hz are compared. It can be seen that CW decoupling (panels a and b) is subject to a larger variation of the residual coupling constant than SHOT decoupling (panels c and d). Comparing parts c and d of Figure 5, the linear SHOT pulse shows the smallest deviations with regard to variations in the actual coupling constant compared to the off-resonance profiles in Figure 2a,b, which were calculated without variations in J. This property of robustness of SHOT decoupling pulses to J variations implies that the actual coupling constant J does not need to be known for the back-calculation of the chemical shift, as long as it falls within a permissible range. Therefore, the reference scans in Figure 3 are in principle not needed, and the experiment can be carried out by recording a single spectrum with SHOT decoupling. The simulations in Figure 5 point out and experiments confirm that J couplings can be scaled either up or down by a SHOT pulse, which is from a theoretical point of view very interesting and currently under further investigation, since so far scaling of J couplings in the literature was limited to reducing the couplings.

However, a deviation of J from J_{opt} comes at the cost of increased sideband amplitudes. Nevertheless, under the conditions used in Figure 5, sidebands do not become larger than the main peaks of the coupled spin. It should further be pointed out that the shown SHOT pulses were so far not specifically optimized for robustness with regard to J variation, which would slow the optimization process significantly. Future improvements of SHOT pulses may be facilitated by more efficient implementation of the optimal control algorithm and parallel computing techniques as well as faster processors. Sidebands might be further decreased by the use of cooperative pulses (COOPs) in combination with SHOT decoupling.[30] COOPs are designed to compensate each other's imperfections in repeated scans.

While off-resonance profiles for CW decoupling are intrinsically not robust with respect to B_1 variations of the decoupling coil, SHOT pulses can be optimized by including an additional cost function, which takes B_1 inhomogeneities into account. All SHOT pulses used here were optimized for B_1 variations of ±2%. To show the robustness of SHOT with regard to B_1 imperfections, a representative decoupled spectrum with a residual peak splitting $J_{SHOT} = J_{opt}/4$ = 40 Hz was simulated for a range of B_1 variations of ±15% (Figure S2 in the Supporting Information). It can be seen that the SHOT pulse does not show a significant change of the peak splitting in the optimized region, and even in the ±15% region shows only slight changes compared to the CW pulse. On the basis of these simulations, chemical shifts obtained from SHOT decoupled experiments are more robust than CW decoupling toward B_1 inhomogeneities. However, increased robustness comes again at the cost of increased sidebands and lowered peak amplitudes.

Since SHOT pulses are only optimized for a certain offset region, a final question arises as to what happens to the spins outside of the optimized bandwidth. Figure S3 in the Supporting Information compares the behavior of the linear SHOT pulse for ^{1}H decoupling, optimized for a 2500 Hz bandwidth, to a CW pulse with $(\gamma/2\pi)B_1$ = 0.5 kHz over a large bandwidth. Outside the optimized region, SHOT pulses have a nondefined off-resonance decoupling pattern, while CW decoupling has the known off-resonance pattern. This indicates

dx.doi.org/10.1021/ac303313s | Anal. Chem. XXXX, XXX, XXX−XXX

that when using SHOT decoupling, it is of particular importance to correctly adjust the center frequency and bandwidth of the pulse.

It is interesting to point out that SHOT pulses achieve the desired offset profile using relatively low rf power. For example, a SHOT pulse that achieves a linear scaling in an offset range of 15 kHz only needs a mean rf amplitude $(\gamma/2\pi)B_{1,\mathrm{RMS}}$ = 0.89 kHz. To achieve a similar off-resonance profile using CW decoupling, an rf amplitude in excess of 10 kHz would be required, which is above the CW power limit of most high-resolution probeheads. SHOT bandwidths higher than 15 kHz have not been optimized yet, and the bandwidth limits are currently under investigation. Low-power SHOT decoupling pulses may further be of interest for hyperpolarized magnetic resonance imaging (MRI), which is subject to more stringent power limitations than high-resolution NMR.

CONCLUSIONS

In summary, we have presented a method for rapid determination of chemical shift correlations applicable to samples hyperpolarized by dissolution DNP. Chemical shifts are reconstructed from an off-resonance decoupling experiment with optimized SHOT pulses, requiring the acquisition of only a one-dimensional spectrum in a single scan. Correlation spectroscopy based on SHOT off-resonance decoupling therefore makes most efficient use of nonrenewable polarization. It circumvents an inherent limitation of the dissolution DNP technique, where noise is introduced with each additional scan into which the originally generated polarization is distributed. SHOT pulses clearly are more complex than most other pulses encountered in traditional NMR experiments. A program has been designed for facile optimization of SHOT pulses yielding specific decoupling profiles and taking B_1 inhomogeneity and power limitations into account. Additionally, due to processor time required for an optimization, pulses are being collected in a library for download and immediate application. Practically, the intricacy in the pulse design translates to a relative simplicity in data analysis. Using a SHOT pulse with a linear decoupling profile, for example, yields residual coupling constants that are proportional to offset from one end of its frequency range. Perhaps more importantly, the decoupling profile of SHOT pulses can be tailored to the specific molecule of interest. This option brings several new applications within reach of this technique. For example, a pulse could be designed to enhance resolution specifically in spectral regions of high signal overlap, such as near the aliphatic and carbonyl resonances in hyperpolarized ^{13}C spectra of peptides. Furthermore, the ability to obtain chemical shift correlations in a single scan may prove beneficial for real-time monitoring of chemical reactions, which requires rapid acquisition of multiple time points.

ASSOCIATED CONTENT

Supporting Information

Additional information as noted in text. This material is available free of charge via the Internet at http://pubs.acs.org.

AUTHOR INFORMATION

Corresponding Author

*E-mail: chilty@chem.tamu.edu.

Author Contributions

§These authors contributed equally to this work.

Notes

The authors declare no competing financial interest.

ACKNOWLEDGMENTS

Financial support from the National Science Foundation (Grant CHE-0846402) and from the Welch Foundation (Grant A-1658) is gratefully acknowledged. F.S. thanks the Fonds der Chemischen Industrie, the Faculty Graduate Center Chemistry, Technical University of Munich (TUM) Graduate School, and the Institute for Advanced Study (IAS) at TUM for financial support. S.J.G. acknowledges support from the Deutsche Forschungsgemeinschaft (DFG; Grant GI 203/6-1) and from the Fonds der Chemischen Industrie.

REFERENCES

(1) Ardenkjær-Larsen, J. H.; Fridlund, B.; Gram, A.; Hansson, G.; Hansson, L.; Lerche, M. H.; Servin, R.; Thaning, M.; Golman, K. *Proc. Natl. Acad. Sci. U.S.A.* **2003**, *100*, 10158−10163.
(2) Hilty, C.; Bowen, S. *Org. Biomol. Chem.* **2010**, *8*, 3361−3365.
(3) Bowen, S.; Hilty, C. *Angew. Chem., Int. Ed.* **2008**, *47*, 5235−5237.
(4) R. Ernst, R.; Bodenhausen, G.; Wokaun, A. *Principles of Nuclear Magnetic Resonance in One and Two Dimensions*; Oxford University Press: Oxford, U.K., 1990.
(5) Frydman, L.; Scherf, T.; Lupulescu, A. *Proc. Natl. Acad. Sci. U.S.A.* **2002**, *99*, 15858−15862.
(6) Mishkovsky, M.; Frydman, L. *Annu. Rev. Phys. Chem.* **2009**, *60*, 429−448.
(7) Zeng, H.; Bowen, S.; Hilty, C. *J. Magn. Reson.* **2009**, *199*, 159−165.
(8) Bloom, J. N.; Shoolery, J. N. *Phys. Rev.* **1955**, *97*, 1261−1265.
(9) Anderson, W. A.; Freeman, R. *J. Chem. Phys.* **1962**, *37*, 85−103.
(10) Ernst, R. *J. Chem. Phys.* **1966**, *45*, 3845−3861.
(11) Reich, H. J.; Jautelat, M.; Messe, M.; Weigert, J.; Roberts, J. D. *J. Am. Chem. Soc.* **1969**, *91*, 7445−7454.
(12) Fesik, S. W.; Eaton, H. L.; Olejniczak, E. T.; Gampe, R. T. *J. Am. Chem. Soc.* **1990**, *112*, 5370−5371.
(13) Grace, C. R.; Riek, R. *J. Am. Chem. Soc.* **2003**, *125*, 16104−16113.
(14) Kwiatkowski, W.; Riek, R. *J. Biomol. NMR* **2003**, *25*, 281−289.
(15) Keller, R.; Grace, C. R. R.; Riek, R. *J. Biomol. NMR* **2006**, *44*, 196−205.
(16) Bowen, S.; Zeng, H.; Hilty, C. *Anal. Chem.* **2008**, *80*, 5794−5798.
(17) Waugh, J. S. *J. Magn. Reson.* **1982**, *50*, 30−49.
(18) Schilling, F.; Glaser, S. *J. Magn. Reson.* **2012**, *223*, 207−218.
(19) Khaneja, N.; Reiss, T.; Kehlet, C.; Schulte-Herbrüggen, T.; Glaser, S. J. *J. Magn. Reson.* **2005**, *172*, 296−305.
(20) Neves, J. L.; Heitmann, B.; Khaneja, N.; Glaser, S. J. *J. Magn. Reson.* **2009**, *201*, 7−17.
(21) Zuiderweg, E. R. P.; Fesik, S. W. *J. Magn. Reson.* **1991**, *93*, 653−658.
(22) Eggenberger, U.; Schmidt, P.; Sattler, M.; Glaser, S. J.; Griesinger, C. *J. Magn. Reson.* **1992**, *100*, 604−610.
(23) McCoy, M. L.; M., A. *J. Magn. Reson., A* **1993**, *101*, 122−130.
(24) Starcuk, Z., Jr.; Bartusek, S. Z., K. *J. Magn. Reson., A* **1994**, *107*, 24−31.
(25) Bendall, M. R. *J. Magn. Reson., A* **1995**, *112*, 26−129.
(26) http://www.org.chemie.tu-muenchen.de/glaser/Downloads.html, accessed 2/13/2013.
(27) Bowen, S.; Hilty, C. *Phys. Chem. Chem. Phys.* **2010**, *12*, 5766−5770.
(28) Harris, R. K.; Becker, E. D.; De Menezes, S. M.; Granger, P.; Hoffman, R. E.; Zilm, K. W. *Magn. Reson. Chem.* **2008**, *46*, 582−598.
(29) Giraudeau, P.; Akoka, S. *J. Magn. Reson.* **2008**, *192*, 151−158.
(30) Braun, M.; Glaser, S. J. *J. Magn. Reson.* **2010**, *207*, 114−123.